Electronic Supplementary Material (ESI) for Food & Function.

Network pharmacology combined with metabolomics and lipidomics to reveal the hypolipidemic mechanism of *Alismatis Rhizoma* in hyperlipidemic mice

Pan Yan[a], Yinyu Wei[a], Meiqin Wang[a], Jianmei Tao[a], Hui Ouyang[c], Zhifeng Du[a], Sen Li[b,*], Hongliang Jiang[a,*]

[a] Tongji School of Pharmacy, Huazhong University of Science and Technology, Wuhan 430030, China;

[b] Department of Pharmacy, Union Hospital, Tongji Medical College, Huazhong University of Science and Technology, Wuhan 430030, China;

[c] Jiangxi University of Traditional Chinese Medicine, Nanchang 330000, China;

*Corresponding author: Sen Li; E-mail: lisentome728@hotmail.com;

*Corresponding author: Hongliang Jiang; E-mail: jianghongliang@hust.edu.cn;

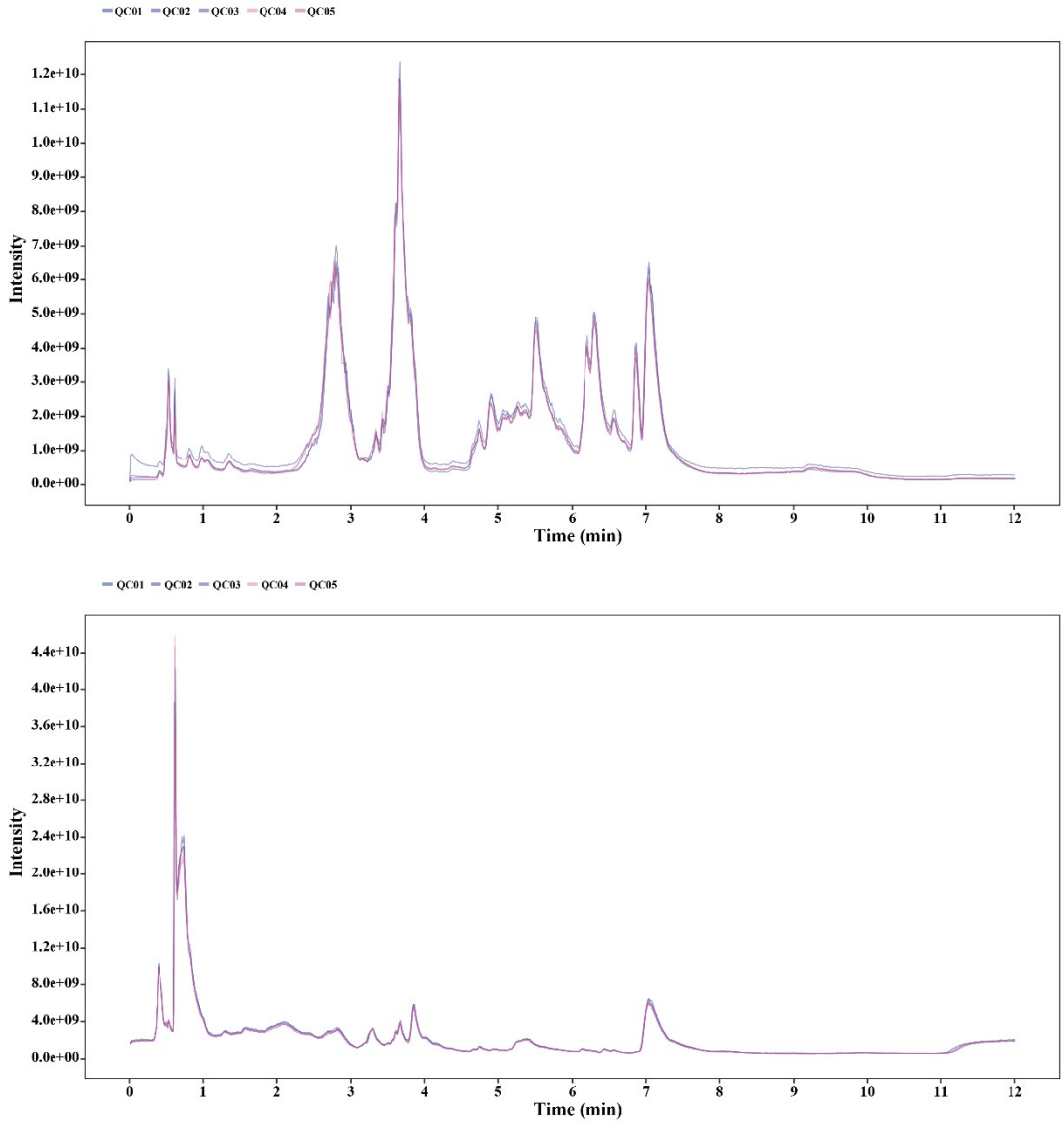

Fig. S1. The overlaid total ion chromatogram of QC in the metabolomics analysis. (A) Positive ion mode, (B) Negative ion mode.

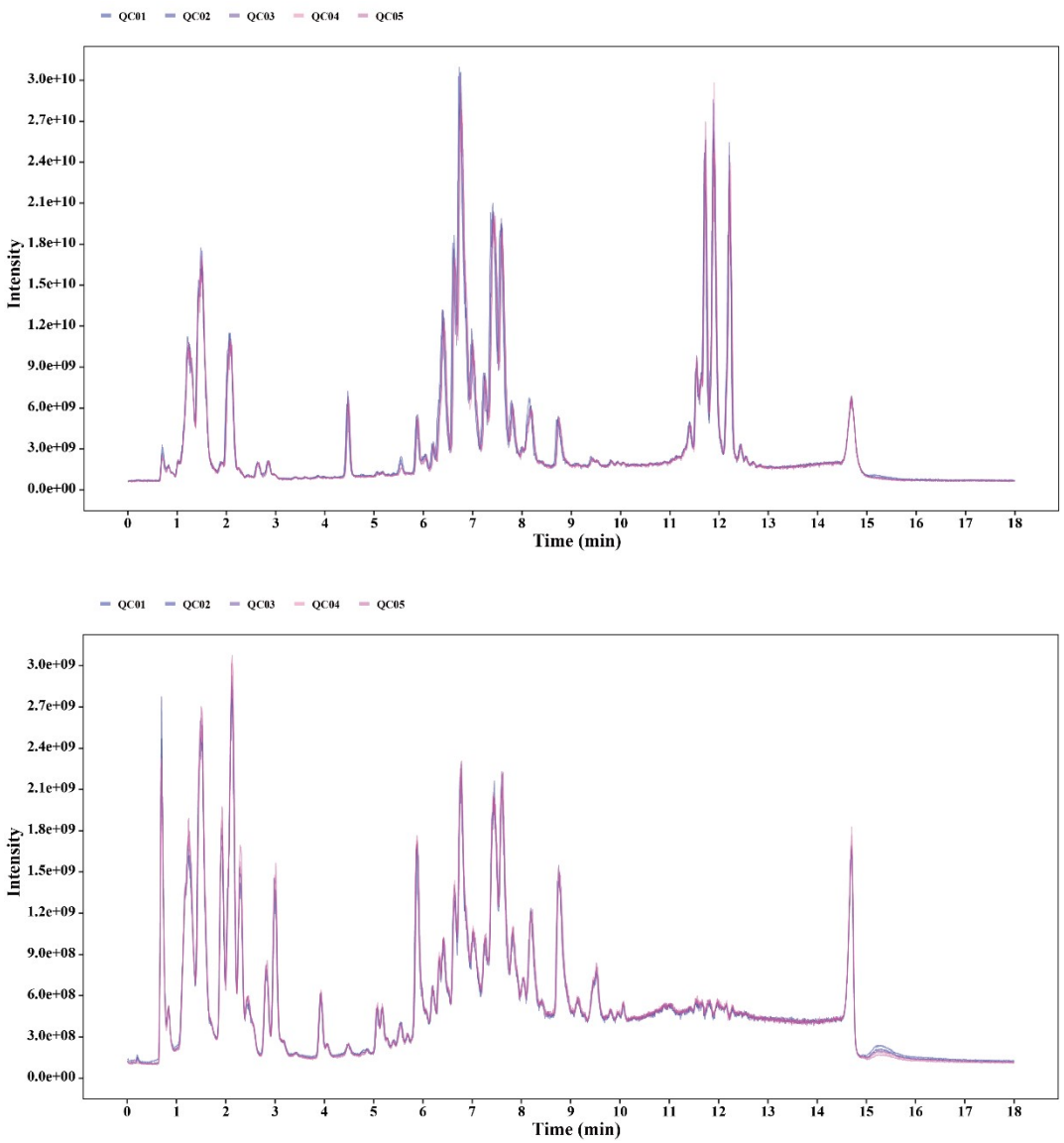

Fig. S2. The overlaid total ion chromatogram of QC in the lipidomics analysis. (A) Positive ion mode, (B) Negative ion mode.

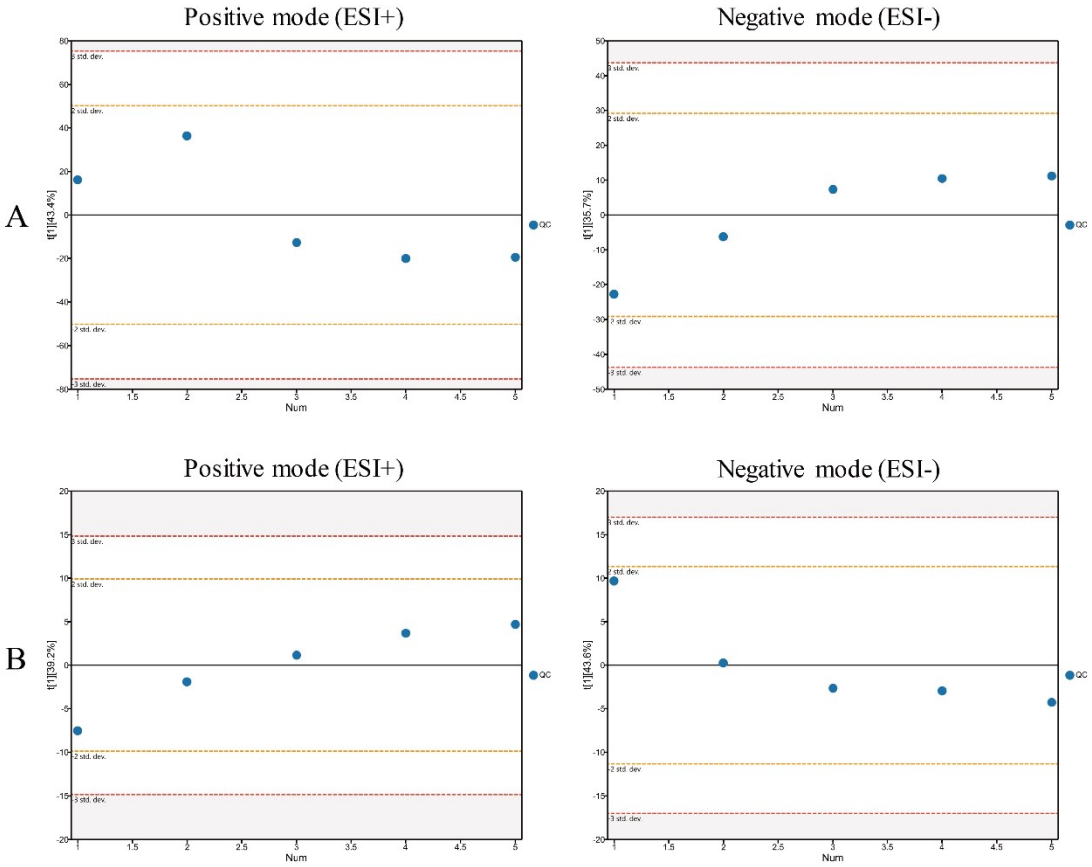

Fig. S3. PCA score plots of QC samples in the (A) metabolomics and the (B) lipidomics analyses.

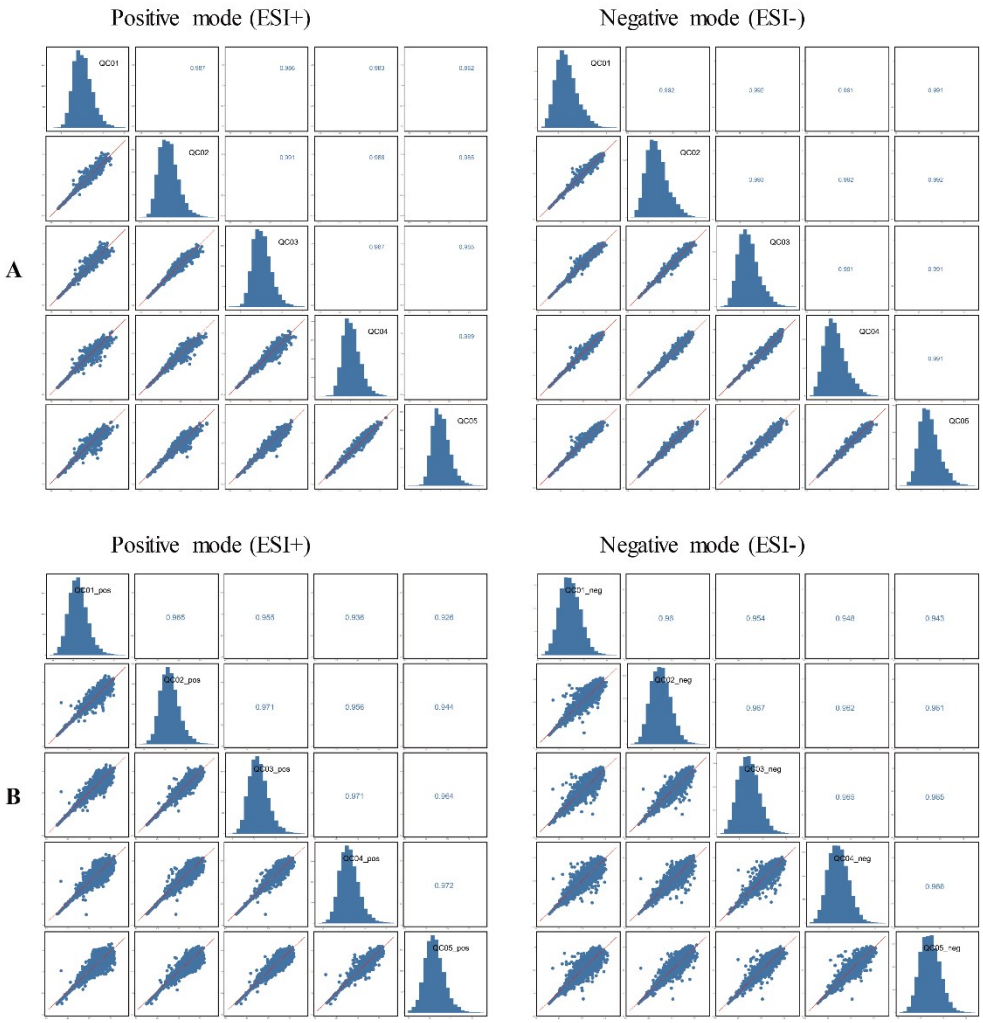

Fig. S4. The correlation of QC samples in the (A) metabolomics and the (B) lipidomics analyses.

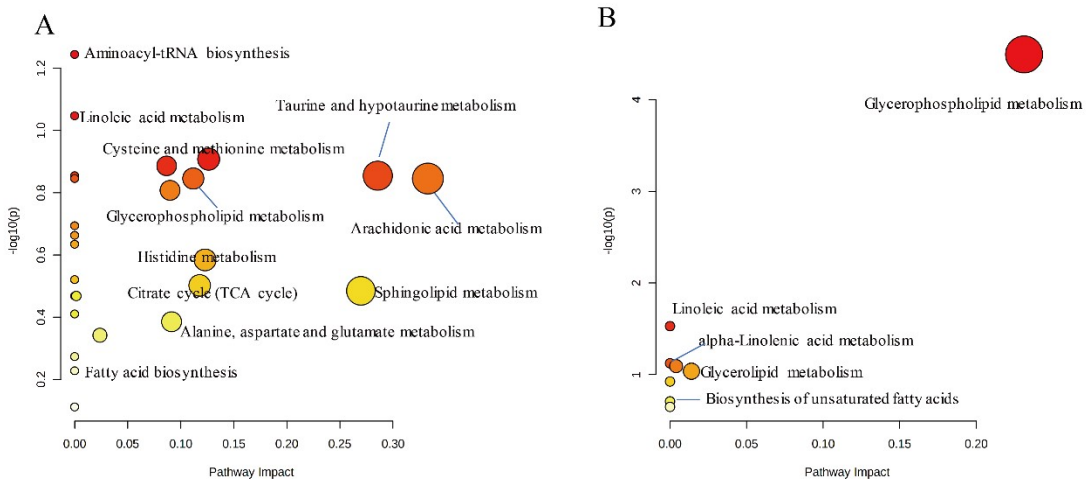

Fig. S5. Pathway analysis of differential metabolites (lipids) from the (A) metabolomics and the (B) lipidomics analyses.

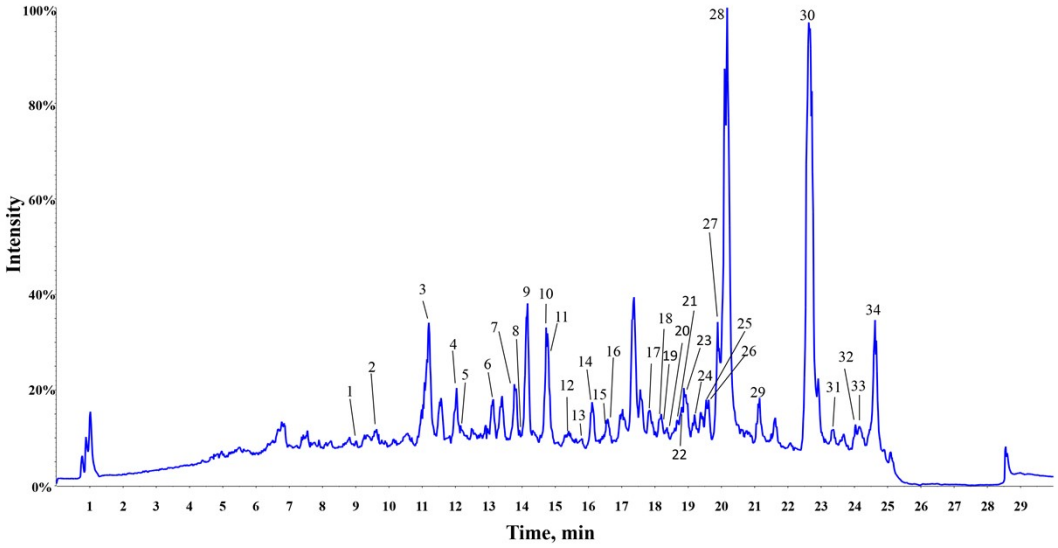

Fig. S6. The TIC of AR extracts in positive mode detected by UHPLC-Q-TOF/MS.

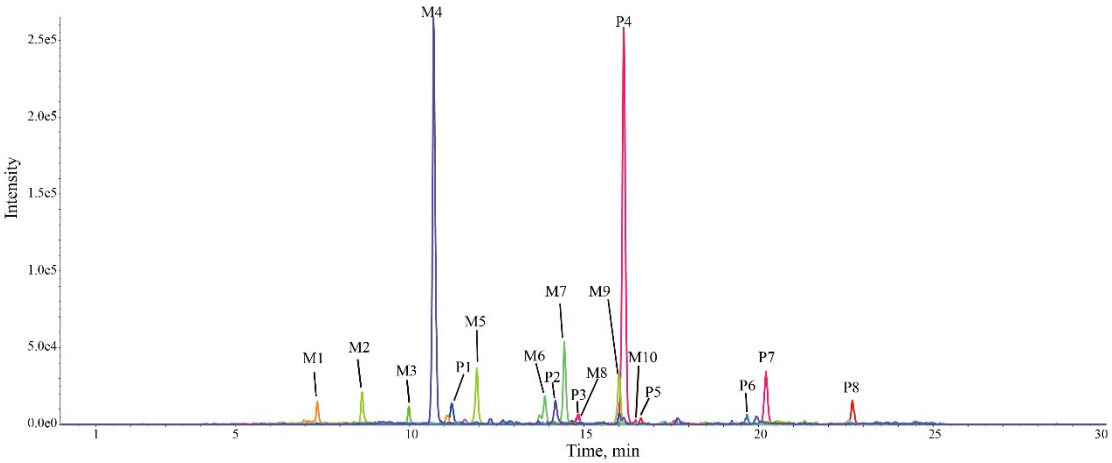

Fig. S7. The XIC of prototypes and metabolites detected in plasma after oral administration of AR.

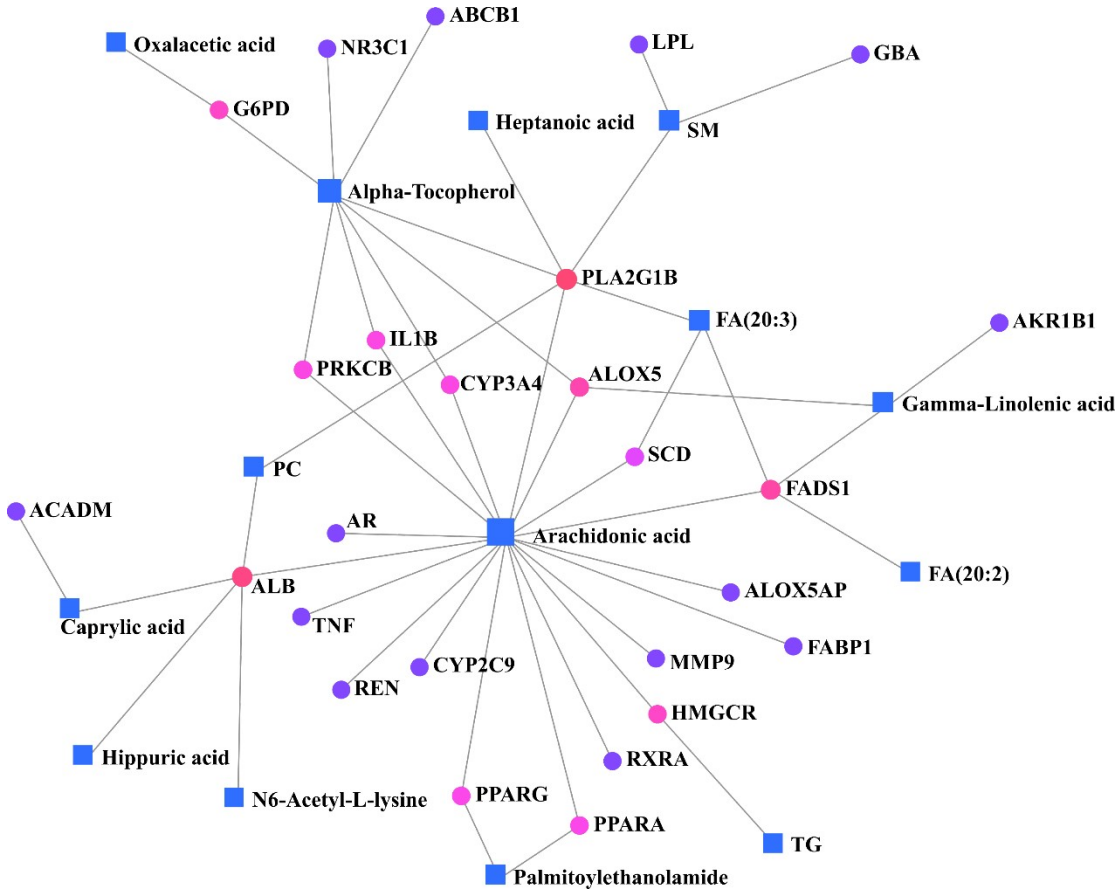

Fig. S8. Gene-Metabolite Interaction Network. The circles represent the genes and the rectangles represent the metabolites and lipids.

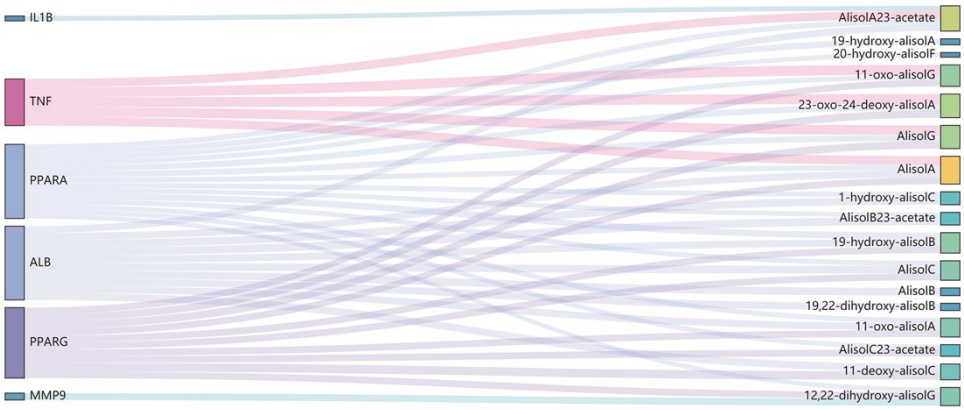

Fig. S9. Sankey diagram between the active compounds and correlated key targets. The thickness of the ribbon is negatively correlated with the docking score.

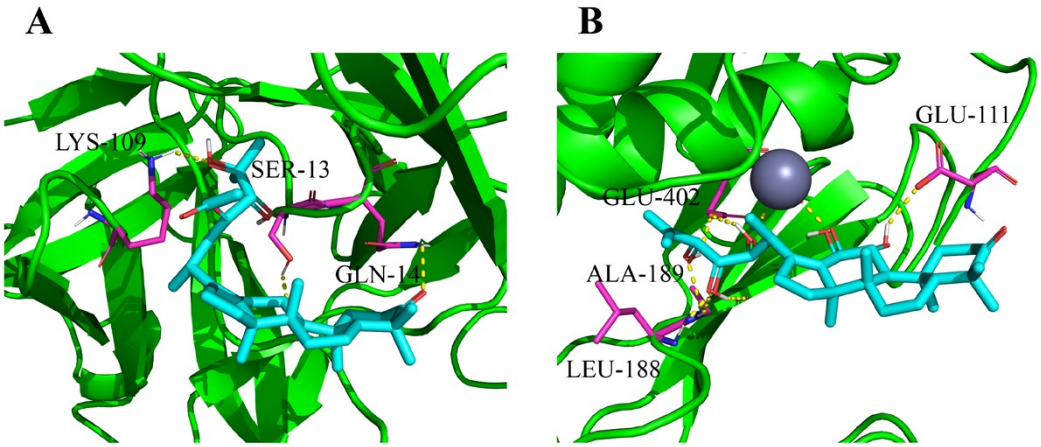

Fig. S10. Docking mode between the alisol A 23-acetate and IL1B (A); Docking mode between the 12,22-dihydroxy-alisol G and MMP9 (B).

Table S1. The nutritional composition of AR powder used in this study.

Composition	Content (per 100 g)
Water	10.1 g
Ashes	2.6 g
Fats	3.8 g
Proteins	22.8 g
Carbohydrates	60.7 g
Na	16.9 mg
K	788 mg
Mg	942 mg
Energy	1560 kJ

Table S2. The primer sequences for qPCR.

Gene	Forward	Reverse
PPARA	TACTGCCGTTTTCACAAGTGC	AGGTCGTGTTCACAGGTAAGA
PPARG	CTCCAAGAATACCAAAGTGCGA	GCCTGATGCTTTATCCCCACA
ALB	CAGCGGAGCAACTGAAGACT	AAGGTTTGGACCCTCAGTCG
MMP9	CTCTCCTGGCTTTCGGCTG	TAGCGGTACAAGTATGCCTCTG
TNF	CCCTCACACTCACAAACCAC	ACAAGGTACAACCCATCGGC
IL1B	GCAGTGGTTCGAGGCCTAAT	GCTGCTTCAGACACTTGCAC
β-actin	CACTGTCGAGTCGCGTCC	TCATCCATGGCGAACTGGTG

Table S3. Food intake of mice fed with AR and simvastatin for 4 weeks.

Week	HFD (g/mouse*day) n=8	SIM (g/mouse*day) n=8	AR (g/mouse*day) n=8
1	6.42 ± 0.89	6.95 ± 1.63	6.75 ± 1.44
2	6.11 ± 0.67	6.81 ± 0.92	6.39 ± 0.95
3	5.53 ± 0.46	5.71 ± 0.76	5.97 ± 0.79
4	5.71 ± 0.93	5.92 ± 0.65	5.66 ± 0.81

Table S4. Metabolic pathways of AR aginst hyperlipidemia in metabolomics analysis.

No	Pathway Name	Match Status	*P*-value	Impact
1	Aminoacyl-tRNA biosynthesis	3/48	0.056953	0
2	Linoleic acid metabolism	1/5	0.089683	0
3	Cysteine and methionine metabolism	2/33	0.12363	0.1263
4	Glycine, serine and threonine metabolism	2/34	0.1299	0.08668
5	Valine, leucine and isoleucine biosynthesis	1/8	0.13972	0
6	Taurine and hypotaurine metabolism	1/8	0.13972	0.28571
7	Biosynthesis of unsaturated fatty acids	2/36	0.14265	0
8	Glycerophospholipid metabolism	2/36	0.14265	0.11182
9	Arachidonic acid metabolism	2/36	0.14265	0.33292
10	Arginine and proline metabolism	2/38	0.15566	0.08992
11	Phenylalanine metabolism	1/12	0.20232	0
12	alpha-Linolenic acid metabolism	1/13	0.21727	0
13	Arginine biosynthesis	1/14	0.23195	0
14	Histidine metabolism	1/16	0.26051	0.12295
15	Pantothenate and CoA biosynthesis	1/19	0.30145	0
16	Citrate cycle (TCA cycle)	1/20	0.3146	0.11782
17	Sphingolipid metabolism	1/21	0.32752	0.26978
18	Pentose phosphate pathway	1/22	0.3402	0
19	Pyruvate metabolism	1/22	0.3402	0.00156
20	Glycolysis / Gluconeogenesis	1/26	0.38865	0
21	Alanine, aspartate and glutamate metabolism	1/28	0.41157	0.09135
22	Glyoxylate and dicarboxylate metabolism	1/32	0.45495	0.02381
23	Valine, leucine and isoleucine degradation	1/40	0.53265	0
24	Fatty acid biosynthesis	1/47	0.59178	0
25	Steroid hormone biosynthesis	1/77	0.77309	0

Table S5. Metabolic pathways of AR aginst hyperlipidemia in lipidomics analysis.

No	Pathway Name	Match Status	*P*-value	Impact
1	Glycerophospholipid metabolism	4/36	3.1904E-5	0.23128
2	Linoleic acid metabolism	1/5	0.029564	0
3	alpha-Linolenic acid metabolism	1/13	0.075253	0
4	Glycosylphosphatidylinositol (GPI)-anchor biosynthesis	1/14	0.080828	0.00399
5	Glycerolipid metabolism	1/16	0.091887	0.01402
6	Sphingolipid metabolism	1/21	0.11902	0
7	Arachidonic acid metabolism	1/36	0.19615	0
8	Biosynthesis of unsaturated fatty acids	1/36	0.19615	0
9	Steroid biosynthesis	1/42	0.22528	0

Table S6. Characterization of prototype compounds of AR extracts based on UHPLC-QTOF-MS/MS.

No.	t_R (min)	Formula	Experimental (m/z)	Calculated (m/z)	Error (ppm)	Characteristics ions	Identification
1	8.99	$C_{30}H_{48}O_6$	505.3524	505.3524	0.1	353.2465	16-oxo-Alisol A
2	9.44	$C_{32}H_{50}O_7$	529.3489*	529.3465	4.5	353.2478	16-oxo-Alisol A 23-acetate
3	11.19	$C_{30}H_{46}O_5$	487.3420	487.3418	0.4	353.2482	Alisol C
4	12.02	$C_{30}H_{46}O_5$	487.3412	487.3418	-1.2	353.2487	11-anhydro-16-oxo-Alisol A
5	12.16	$C_{30}H_{48}O_5$	489.3561	489.3575	-2.8	355.2635	11-deoxy-16-oxo-Alisol A
6	13.13	$C_{32}H_{50}O_6$	513.3573*	513.3575	-0.3	381.2788, 337.2526	16-acetoxy-Alisol B
7	13.80	$C_{32}H_{50}O_7$	547.3621	547.3629	-1.5	381.2779, 337.2527	16-hroperoxyalisol B 23-acetate
8	14.00	$C_{30}H_{48}O_5$	471.3465*	471.3469	-0.8	381.2787, 339.2674	Alisol F
9	14.16	$C_{32}H_{48}O_6$	529.3525	529.3524	0.3	353.2484	Alisol C 23-acetate
10	14.77	$C_{30}H_{46}O_4$	471.3466	471.3469	-0.6	355.2637	11-deoxy-Alisol C
11	14.86	$C_{30}H_{44}O_4$	469.3314	469.3312	0.3	353.2474	Alisol L
12	15.29	$C_{32}H_{50}O_6$	513.3572*	513.3575	-0.5	381.2787, 339.2684	Alisol F 24-acetate
13	15.98	$C_{32}H_{46}O_6$	527.3341	527.3367	-5.0	369.2449	Alisol K 23-acetate
14	16.13	$C_{30}H_{50}O_5$	473.3621*	473.3625	-0.9	383.2952, 339.2687	Alisol A
15	16.56	$C_{30}H_{46}O_4$	453.3366*	453.3363	0.6	381.2798, 339.2694	16,23-oxido-Alisol B
16	16.62	$C_{32}H_{52}O_6$	515.3729*	515.3731	-0.4	383.2953, 339.2683	Alisol A 23-acetate
17	17.97	$C_{32}H_{50}O_6$	531.3661	531.3680	-3.6	355.2546	Alismaketone A 23-acetate
18	18.15	$C_{32}H_{52}O_6$	515.3726	515.3731	-1.0	383.2952, 339.2689	Alisol A 24-acetate
19	18.20	$C_{32}H_{50}O_6$	531.3674	531.3680	-1.2	355.2655	Alisol D
20	18.35	$C_{32}H_{46}O_5$	511.3403	511.3418	-2.9	353.2472	Alisol L 23-acetate
21	18.79	$C_{32}H_{50}O_6$	531.3677	531.3680	-0.6	381.2785, 337.2522	16-hydroxy-Alisol B 23-acetate
22	18.80	$C_{30}H_{44}O_4$	469.3308	469.3312	-0.9	379.2635, 339.2693	Alismanol E

Table S6. (*continued*)

No.	t_R (min)	Formula	Experimental (m/z)	Calculated (m/z)	Error (ppm)	Characteristics ions	Identification
23	18.90	$C_{32}H_{48}O_5$	513.3573	513.3575	-0.3	355.2634	11-deoxy-Alisol C 23-acetate
24	19.12	$C_{30}H_{46}O_4$	471.3459	471.3469	-2.1	381.2790, 339.2669	24-deacetyl-Alisol O
25	19.62	$C_{30}H_{46}O_4$	471.3467	471.3469	-0.4	381.2774, 339.2674	25-anhydro-Alisol F
26	19.63	$C_{30}H_{48}O_4$	455.3522*	455.3520	0.5	383.2949, 339.2684	Alisol G
27	19.89	$C_{32}H_{50}O_6$	531.3675	531.3680	-1.0	355.2637	Alisol N 23-actate
28	20.15	$C_{30}H_{48}O_4$	455.3513*	455.3520	-1.5	383.2939, 339.2683	Alisol B
29	21.13	$C_{32}H_{48}O_5$	513.3574	513.3575	-0.1	381.2795, 339.2680	Alisol O
30	22.66	$C_{32}H_{50}O_5$	515.3721	515.3731	-1.9	383.2950, 339.2685	Alisol B 23-acetate
31	23.35	$C_{30}H_{46}O_4$	471.3465	471.3469	-0.8	3812791, 339.2693	Alismanol Q
32	24.15	$C_{30}H_{46}O_3$	455.3519	455.3520	-0.2	383.2942, 339.2677	Alisol X
33	24.18	$C_{30}H_{44}O_3$	453.3365	453.3363	0.4	381.2799, 339.2689	11,25-anhydro-Alisol F
34	24.64	$C_{30}H_{48}O_3$	457.3674	457.3676	-0.5	385.3103, 341.2841	11-deoxy-Alisol B

*: dehydrated form of compound was detected as the major peak in MS because dehydration in-source occurs easily, and the peak of undehydrated compound was too weak to get enough MS/MS fragments, therefore identification was based on MS/MS fragments of dehydrated form.

Table S7. Characterization of prototypes and metabolites of AR triterpenes in plasma based on UHPLC-QTOF-MS/MS.

No.	Name	RT (min)	Experimental m/z	Calculated m/z	Error (ppm)	Characteristic ions	Formula
P1[#]	Alisol C	11.21	487.3413	487.3418	-1.0	353.2496	$C_{30}H_{46}O_5$
P2[#]	Alisol C 23-acetate	14.18	529.3518	529.3524	-1.1	353.2485	$C_{32}H_{48}O_6$
P3	11-deoxy alisol C	14.81	471.3485	471.3469	3.4	355.2636	$C_{30}H_{46}O_4$
P4[#]	Alisol A	16.14	473.3625*	473.3626	0.1	383.2952, 339.2690	$C_{30}H_{50}O_5$
P5[#]	Alisol A 23-acetate	16.63	515.3731*	515.3717	-2.7	339.2688	$C_{32}H_{52}O_6$
P6[#]	Alisol G	19.67	455.3517*	455.3520	-0.7	383.2935, 339.2728	$C_{30}H_{48}O_4$
P7[#]	Alisol B	20.21	455.3528*	455.3520	1.8	383.2954, 339.2683	$C_{30}H_{48}O_4$
P8[#]	Alisol B 23-acetate	22.69	515.3731	515.3725	3.9	383.2964, 339.2696	$C_{32}H_{50}O_5$
M1	1-hydroxy-alisol C	7.35	503.3362	503.3367	-1.1	351.2315	$C_{30}H_{46}O_6$
M2	20-hydroxy-alisol F	8.64	505.3517	505.3524	-1.3	379.2631, 337.2559	$C_{30}H_{48}O_6$
M3	Alisol C 23-acetate-11-O-GluA	9.98	705.3810	705.3844	-4.9	529.3494	$C_{38}H_{56}O_{12}$
M4	19-hydroxy-alisol A	10.70	507.3674	507.3680	-1.2	381.2788, 337.2525	$C_{30}H_{50}O_6$
M5	19,22-dihydroxy-alisol B	11.93	505.3518	505.3524	-1.2	379.2593, 337.2492	$C_{30}H_{48}O_6$
M6	11-oxo-alisol A	13.71	489.3565	489.3574	-1.9	355.2654	$C_{30}H_{48}O_5$
M7	19-hydroxy-alisol B	14.43	489.3570	489.3574	-1.0	381.2780, 337.2532	$C_{30}H_{48}O_5$
M8	23-oxo-24-deoxy-aliosl A	14.84	473.3613	473.3625	-2.6	383.2978, 339.2641	$C_{30}H_{48}O_4$
M9	12,22-dihydroxy-alisol G	15.99	505.3517	505.3524	-1.4	355.2654	$C_{30}H_{48}O_6$
M10	11-oxo-alisol G	16.55	471.3467	471.3469	-0.4	355.2627	$C_{30}H_{46}O_4$

*: dehydrated form of compound was detected as the major peak in MS because dehydration in-source occurs easily, and the peak of undehydrated compound was too weak to get enough MS/MS fragments, therefore identification was based on MS/MS fragments of dehydrated form; P: prototypes; M: metabolites; [#]: confirmed with reference standards.

Table S8. The hub genes filtrated from PPI by CytoHubba.

Gene symbol	MCC	MNC	Degree	EPC	BottleNeck	EcCentricity	Closeness	Radiality	Betweenness	Stress
ALB	45823894	53	53	25.648	9	0.33333	66.83333	4.71605	1037.153	5832
TNF	45824123	51	52	25.037	33	0.25	66.08333	4.67901	878.288	4770
PPARG	40423970	44	44	24.412	2	0.25	62.08333	4.58025	468.5296	3146
PPARA	131746	41	41	23.266	10	0.25	60.58333	4.54321	521.7559	3470
EGFR	45692162	35	35	22.846	1	0.25	57.41667	4.45679	304.0837	2304
IL1B	45120696	33	33	21.808	1	0.25	56.08333	4.40741	174.2581	1396
IGF1	45691728	31	31	21.451	1	0.25	55.41667	4.40741	133.3232	1172
FASN	196256	28	28	20.366	2	0.25	54.08333	4.38272	242.1478	1818
ESR1	4974902	27	27	19.706	1	0.25	53.25	4.34568	105.0921	888
MMP9	45147050	25	25	18.952	2	0.25	52.08333	4.30864	72.80311	600

Table S9. KEGG enrichment analysis of 83 genes.

No	Pathway	*P*-value
1	PPAR signaling pathway	3.04E-08
2	Regulation of lipolysis in adipocytes	1.9E-06
3	Insulin resistance	1.96E-06
4	Prostate cancer	3.96E-05
5	AMPK signaling pathway	4.67E-05
6	HIF-1 signaling pathway	6.94E-05
7	Hepatitis C	8.15E-05
8	Non-alcoholic fatty liver disease (NAFLD)	0.000198
9	Pathways in cancer	0.000244
10	Proteoglycans in cancer	0.000267
11	Non-small cell lung cancer	0.000313
12	Renin secretion	0.000585
13	Calcium signaling pathway	0.000625
14	Estrogen signaling pathway	0.000642
15	Neuroactive ligand-receptor interaction	0.000699
16	Bile secretion	0.000827
17	TNF signaling pathway	0.000967
18	PI3K-Akt signaling pathway	0.001047
19	Thyroid hormone signaling pathway	0.001407
20	cGMP-PKG signaling pathway	0.001462
21	Ovarian steroidogenesis	0.001813
22	Ras signaling pathway	0.00279
23	mTOR signaling pathway	0.003376
24	Central carbon metabolism in cancer	0.004818
25	Chagas disease (American trypanosomiasis)	0.005059
26	Pancreatic cancer	0.005092
27	Glioma	0.005092
28	cAMP signaling pathway	0.005188
29	Adipocytokine signaling pathway	0.006624
30	Prolactin signaling pathway	0.006963
31	Rap1 signaling pathway	0.007116
32	Metabolism of xenobiotics by cytochrome P450	0.00805
33	Aldosterone-regulated sodium reabsorption	0.008274
34	Sphingolipid signaling pathway	0.009185
35	Osteoclast differentiation	0.0131
36	Measles	0.013916
37	ErbB signaling pathway	0.01403
38	Fatty acid metabolism	0.014619
39	Insulin signaling pathway	0.016106
40	Endometrial cancer	0.018119
41	Hepatitis B	0.019543

Table S9 (*continued*)

No	Pathway	*P*-value
42	Inflammatory mediator regulation of TRP channels	0.020852
43	NOD-like receptor signaling pathway	0.022046
44	Acute myeloid leukemia	0.022046
45	T cell receptor signaling pathway	0.022277
46	Focal adhesion	0.022956
47	Amoebiasis	0.026905
48	Toll-like receptor signaling pathway	0.026905
49	Arachidonic acid metabolism	0.027557
50	VEGF signaling pathway	0.027557
51	Apoptosis	0.02874
52	Toxoplasmosis	0.030289
53	Serotonergic synapse	0.031172
54	Inflammatory bowel disease (IBD)	0.031186
55	Transcriptional misregulation in cancer	0.033378
56	Fc epsilon RI signaling pathway	0.036395
57	Drug metabolism - cytochrome P450	0.036395
58	Complement and coagulation cascades	0.037763
59	Linoleic acid metabolism	0.038442
60	Influenza A	0.038801
61	Melanoma	0.040577
62	Graft-versus-host disease	0.048643
63	African trypanosomiasis	0.048643

Table S10. The docking scores between 6 key targets and the corresponding components.

Protein	PDB	Small molecule	Docking score (kcal/mol)
ALB	1AO6	Alisol A	-7.8
ALB	1AO6	11-deoxy-alisol C	-8.0
ALB	1AO6	Alisol A 23-acetate	-7.4
ALB	1AO6	Alisol B	-8.4
ALB	1AO6	Alisol B 23-acetate	-8.6
ALB	1AO6	Alisol C	-8.4
ALB	1AO6	1-hydroxy-alisol C	-8.5
ALB	1AO6	19-hydroxy-alisol B	-7.9
ALB	1AO6	19,22-dihydroxy-alisol B	-7.8
ALB	1AO6	11-oxo-alisol A	-7.7
ALB	1AO6	19-hydroxy-alisol B	-7.9
TNF	7KPA	Alisol A	-9.6
TNF	7KPA	Alisol A 23-acetate	-9.1
TNF	7KPA	Alisol G	-10.4
TNF	7KPA	23-oxo-24-deoxy-alisol A	-10.9
TNF	7KPA	11-oxo-alisol G	-10.8
IL1B	1ITB	Alisol A 23-acetate	-5.3
MMP9	1GKC	12,22-dihydroxy-alisol G	-7.5
PPARG	6TSG	Alisol A	-7.2
PPARG	6TSG	Alisol C	-7.3
PPARG	6TSG	Alisol C 23-acetate	-7.4
PPARG	6TSG	Alisol G	-8.3
PPARG	6TSG	11-deoxy-alisol C	-9.2
PPARG	6TSG	19-hydroxy-alisol B	-7.3
PPARG	6TSG	11-oxo-alisol A	-7.4
PPARG	6TSG	23-oxo-24-deoxy-alisol A	-8.2
PPARG	6TSG	12,22-dihydroxy-alisol G	-7.4
PPARG	6TSG	11-oxo-alisol G	-7.2
PPARA	5HYK	Alisol A	-5.8
PPARA	5HYK	Alisol A 23-acetate	-5.8
PPARA	5HYK	Alisol B 23-acetate	-5.1
PPARA	5HYK	Alisol C	-5.5
PPARA	5HYK	Alisol C 23-acetate	-5.3
PPARA	5HYK	Alisol G	-6.6
PPARA	5HYK	1-hydroxy-alisol C	-5.6
PPARA	5HYK	20-hydroxy-alisol F	-5.1
PPARA	5HYK	19-hydroxy-alisol A	-6.6
PPARA	5HYK	11-oxo-alisol A	-5.4

Table S10 (*continued*)

Protein	PDB	Small molecule	Docking score (kcal/mol)
PPARA	5HYK	19-hydroxy-alisol B	-7.1
PPARA	5HYK	23-oxo-24-deoxy-alisol A	-6.7
PPARA	5HYK	12,22-dihydroxy-alisol G	-4.9
PPARA	5HYK	11-oxo-alisol G	-5.4